Characterization of Low-CO_2 Ferrite-Belite Cements Incorporating High Volumes of Bauxite Residue as a Raw Material

Rahul Roy[1], Tobias Hertel[2] and Yiannis Pontikes[3]
1. PhD student
2. Post-doctoral researcher
3. Professor of Sustainable Resources for Engineered Materials (SREMat)
Department of Materials Engineering, KU Leuven, Kasteelpark Arenberg 44, Leuven, Belgium
Corresponding author: rahul.roy@kuleuven.be

Abstract

Bauxite residue (BR) is the main waste of the alumina sector. It is produced at rates of 170 million tons per year, out of which only 4 million tonnes are used in other industrial processes. Currently, less than 3 % is used as a raw material in Portland cement production, mostly due to limitations imposed by the clinker chemistry itself. Hence, research is being carried out to develop Fe-rich cements, and by doing so, incorporate higher levels of BR. In the work herein, a low-CO_2 ferrite-belite cement clinker was developed by incorporating more than 35 wt% BR as a raw material. Two sets of clinker mixtures were designed using thermodynamic modelling, and limestone, kaolin, and BR as raw materials. A low-BR clinker (38 wt% BR) and a high-BR clinker (50 wt% BR) were synthesized at 1250-1260°C, followed by rapid cooling. The results obtained from quantitative X-ray diffraction and electron probe microanalysis indicated that the low-BR content clinker had more $Ca_2(Al_xFe_{1-x})_2O_5$ and C_2S (reactive phases) with some minor gehlenite, whereas a higher BR content increased the content of gehlenite and perovskite. Apart from the particular phase assemblage and the amount of each phase formed, the amount of BR in the clinker's raw meal also affects the particular solid solutions formed. This is due to the variability in the Al/Fe ratio in the $Ca_2(Al_xFe_{1-x})_2O_5$ phase influencing the reactivity, but also due to the presence of Na^+, transition metals such as Fe^{3+} and Ti^{2+} in the $Ca_2(Al_xFe_{1-x})_2O_5$ as well as C_2S reactive phases , being able to stabilize the reactive polymorphic phases. In addition, an interstitial face such as reactive mayenite is formed at lower temperatures due to rapid cooling. Moreover, it is also expected that the solidification path will play a role, and that higher cooling rates will most likely lead to enhanced overall hydraulic activity.

Keywords: Bauxite residue, Clinker, Ferrite-belite cement, Rapid cooling, Reactivity, Stabilize

1. Introduction

The utilization of BR is roughly about 10 % in China and 2-3% globally [1]. The use of bauxite residue in the manufacturing of construction materials is a path of considerable interest for the alumina producer since it may absorb vast amounts of waste and provide a new revenue stream. Few alumina refineries in the world such as Hindalco in India, Mykolaiv in Ukraine and Mytilineos in Greece are supplying unmodified-BR as a raw material to the cement plant for Portland cement production (OPC). Hindalco achieved an 100% utilization of bauxite residue from three of its refineries by sending it to more than 40 cement plants in India, achieving a sale of 2 million tonnes of its BR production [2]. It is estimated that a total of 3 million tonnes of BR are used in the production of clinker worldwide. However, the use of BR as a raw material component in the OPC production varied between 0.8-3.5 wt.% [3]. Low-valorization values of BR has encouraged various organizations such as the International Alumina Institute to reach the strategic target goal of 20% valorization of BR by 2025.

Currently in the laboratory scale, more than 20% of BR has been successfully valorized in the production of cements. In one of the research works, the amount of BR that has been valorized

accounted up to 23 wt.% in the raw meal production of OPC [4]. In this work, dealkalized BR obtained from the sintering process was used instead of the Bayer process. The dealkalized BR accounted for higher content of CaO and SiO_2, thus making it suitable for large quantities allocated in the raw meal of OPC. BR has also found its ways as a raw material in the production of inorganic polymers. In the recent works of Giels et al. [5], a compressive strength of 131MPa was achieved in 28 days by incorporating 81 wt% of BR. The BR was thermally modified at 1200–1300 °C with minor additions of C, CaO and SiO2 to develop a reactive precursor. Thus, opening the possibility of upscaling the work. In the production of calcium sulfo-ferroaluminate cements (CSA-F), the maximum amount of BR valorized in the clinker production was 65 wt.% [6], nevertheless the highest 2 days compressive strength achieved was 28.5 MPa which is comparatively lower than the market produced standard CSA cements but still better than OPC 52.5N. In the works of Hertel et al. [7], a 35.5 wt% BR as a raw meal component of CSA cement achieved a 2d compressive strength of 43MPa almost similar to the market produced CSA cements. In the production of ferrite-belite cements, incorporation high volumes of BR > 30 wt % to achieve a considerable compressive strength is still in progress. Currently, Montoya et al. [8] only achieved a compressive strength of 10 MPa after 28 days. Hence to understand the poor compressive strength results, it is important to characterize the clinker phase composition in depth.

To achieve a clinker replacement factor of 30 wt% and a strength activity index above 75%, the EU-funded project - ReActiv (Industrial Residue Activation for Sustainable Cement Production) was implemented to achieve this milestone. In this study, two types of clinkers were produced from limestone (LS), kaolin (K) and bauxite residue (BR), with clinker replacement of 38 wt% and 50 wt% with BR at a chosen clinkering temperature range between 1250-1260°C followed by rapid cooling respectively [9]. The first step of evaluating these clinkers was to characterize them. The minerology of the produced clinkers was obtained by X-ray diffraction (XRD). In addition, the X-ray fluorescence (XRF), scanning electron microscope (SEM-EDX) and electron probe micro-analysis (EPMA) was used for characterization. The physical characterizatin of the clinker was accomplished by measuring the density, blaine fineness and the particle size distribution.

2. Materials and Methods

2.1 Production of Clinker

The raw materials for the ferrite-belite (FB) clinker were limestone (Carmeuse), bauxite residue (Mytilineos) and Kaolin (Imerys). Two mixtures of the FB cements were chosen: (1) LS57BR38CL5 where, 57 wt% of LS was mixed with 38 wt% BR and 5 wt% K and (2) LS45BR50CL5 where, 45 wt% of LS was mixed with 50 wt% BR and 5 wt% K.

Figure 1 represents the schematic representation of the process flow for the preparation of the selected mixtures, based on the modification of the work of Montoya et al. [8].The weighed raw materials were mixed with ethanol and (a) zirconia grinding elements for 12 hr in an overhead shaker (Turbula WAB T2F) to obtain a homogeneous blend. (b) The mixtures were dried using rotovap (Heidolph 4010) to remove the ethanol. (c) The dried mixture for each selected composition mixed with 15% deionized water in a Hobart mixer to form ~ 2cm spherical pellets by hand. To remove the excess water content, the pellets were dried at 110°± 5 °C for 24h using a drying oven (Binder ED 260).

Figure 2 represents the schematic representation of the process flow for clinker production of the selected mixture. The pellets were placed in an (a) alumina crucible and (b) introduced in a bottom-loading furnace (AGNI ELT 160-02) to reach the target temperature of 1260°C at a rate

of 10°C/min, followed by an isothermal step of 60 min at 1260°C in order to increase the belite content and consume the formed gehlenite at low temperatures [10]. Finally, the heating process was terminated, and the clinker was quenched rapidly using (c) air gun. The obtained clinker was ground in a vibratory ring mill (Retsch RS200) and a blaine fineness of 4000 cm^2/g was targeted similar to OPC clinkers .

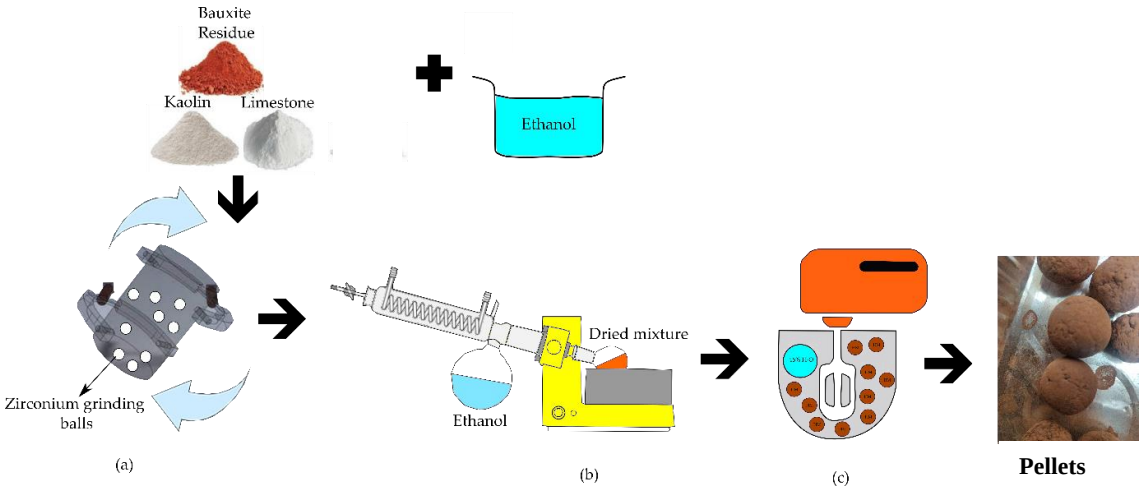

Figure 1. Schematic representation of the process flow for preparation of the selected clinker mixtures.

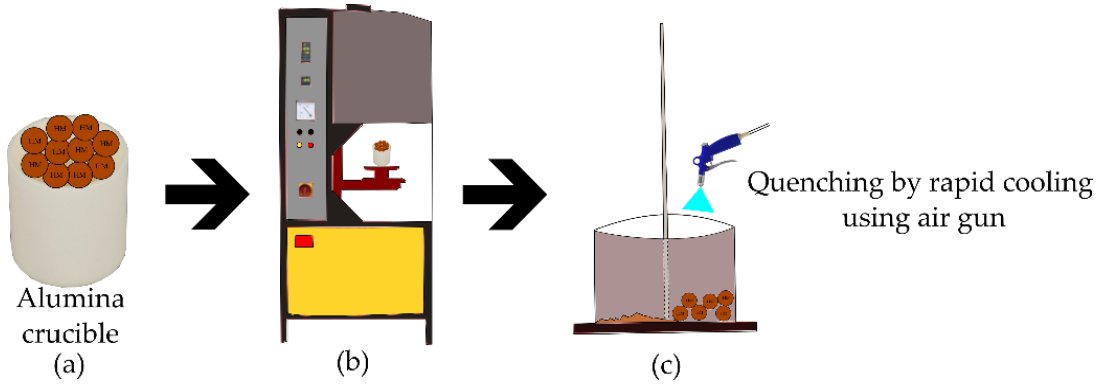

Figure 2. Schematic representation of the process flow for clinker production of selected mixture

2.2 Chemical and Mineralogical Characterization of Clinker

The chemical composition of the clinker was obtained using XRF (Bruker S8 Tiger 4 kW Rh system). Qualitative and Quantitative XRD was measured using a D2 Phaser diffractometer subjected to a CuKα radiation with tube settings at an accelerating voltage of 30 kV and a current of 10 mA. The samples were scanned in the 2θrange of 5–65° with a step size of 0.02° and at a rate of 0.7 sec per step for data collection. In the quantitative analysis, the samples were prepared in triplicates with 10 wt% analytical grade ZnO as an internal standard, followed by wet milling (ethanol) in a custom-made micronizing McCrone mill for 5 min [11]. The milled samples were kept in fumehood for 24 h for the ethanol to evaporate, followed by oven-drying at a temperature of 110°C± 5 °C for 30 min. After drying, the samples were ground using mortar and pestle to pass through 80micron sieve. The software DiffracEVA V4.1 (structures using the ICDD PDF2 database) and TOPAS-Academic V5 (structures from ICDD database) were used for qualitative and quantitative analysis, respectively. Table 1 enlists the phases used in the Rietveld analysis.

Table 1. ICDD-PDF and ICSD collection codes for all phases used for Rietveld refinements.

Clinker Phase	Terminology	PDF code	ICSD code	Ref.
Brownmillerite - $Ca_2(Al,Fe)_2O_5$	C_4AF	30-0226	9197	[12]
Larnite - Ca_2SiO_4	C_2S	09-0351	39006	[13]
Gehlenite - $Ca_2Al_2SiO_7$	C_2AS	09-0216	39921	[14]
Mayenite - $Ca_{12}Al_{14}O_{33}$	$C_{12}A_7$	09-0413	6287	[15]
Perovskite – $CaTiO_3$	CT	77-0182	37263	[16]

To visualize the clinker phases and distinguish them based on their appearance, scanning electron microscope (Philips XL30 FEG) was incorporated. Moreover, energy-dispersive spectroscopy (EDS) was adopted to determine the stoichiometry of the Al_2O_3/ Fe_2O_3 (A/F) in the ferritic phase of the clinker. The samples were ground and polished using 3 µm and 1 µm oil-based suspensions. Thereafter, the sample was coated with a 2 nm Pt coating and carbon glue on the sides of the resin was added to ensure conductivity. Before the analysis, the samples were degassed in a vacuum chamber for 24 h. The samples were analyzed at an accelerating voltage between 15-20 KV and EDX spot analysis was performed at the area of interest.

EPMA (JEOL JXA-8530F) was carried out on clinker to determine the chemical composition of the phases. An accelerating voltage of 15 kV, a probe current of 15 nA and a defocused beam of 2 µm were used. Analysis results outside the range of 98 to 102 % before normalisation were not considered. Ten measurements per phase were taken and results were averaged. The measured elements, the standards used, and the analysing crystals are listed in Table 2.

Table 2. Measured elements, standards and analysing crystals for EPMA WDS analysis. 15 kV, 50 nA and 2 µm defocused beam. The standards were provided by SPI supplies (USA).

Measured elements	Oxide normalisation	Standard	Analysing Crystal	X-ray line
Al	Al_2O_3	Plagioclase_An65	TAP	Al Kα
Ti	TiO_2	Rutile	PETJ	Ti Kα
Fe	Fe_2O_3	Haematite	LIF	Fe Kα
Na	Na_2O	Plagioclase_An65	TAPH	Na Kα
Si	SiO_2	Diopside	PETH	Si Kα
Ca	CaO	Diopside	PETH	Ca Kα

3. Results and Discussions

3.1 Chemical Composition of Clinker

The chemical composition of the clinkers by XRF on glass beads is listed in Table 3. In comparison to OPC, FB clinkers had 18-22 % and 10-12 % more Fe_2O_3 and Al_2O_3 content respectively. Moreover, due to the presence of BR in these iron-rich clinker, the TiO_2 content was 3-4 % higher than the OPC. However, the CaO and SiO_2 content was comparatively lower than the OPC. The silica ratio expressed as SiO_2/ (Al_2O_3 + Fe_2O_3) was 2.7 for OPC whereas for the FB cements it was approximately between 0.18-0.21. This indicates that the presence of lower silica ratio in the FB cements is expected to lead to more of aluminates and ferrites than calcium silicates. Furthermore, a lower A/F ratio in FB clinkers i.e., less than 1 means there is a probability of more Fe-rich ferrite phases which can influence the setting time of the pastes [17].

Table 3. XRF analysis of prepared clinkers and OPC. The values are given in %.

	OPC	LS57BR38CL5	LS45BR50CL5
Oxides		**Glass bead**	**Glass bead**
CaO	64.4	50.0	39.6
SiO_2	21.38	7.82	8.62
Al_2O_3	4.97	15.6	18.8
Fe_2O_3	2.93	20.6	25.8
SO_3	3.14	0.27	0.29
TiO_2	0.24	2.85	3.58
MgO	1.01	0.26	0.24
Na_2O	0.30	1.97	2.46
K_2O	0.86	-	-
P_2O_5	0.26	0.12	0.00
Cl	0.00	-	-
Total	99.01	99.61	99.39

3.2 Mineralogy of the Produced Clinkers

Based on the qualitative analysis of the selected FB cement clinkers in comparison to OPC (Figure 3), peaks of C_2S were more prominent in the iron-rich ferrite-belite clinker This indicates that at lower temperature (1260°C), the amount of C_2S formed is higher in FB clinker due to absence of melt which draws the reactant particles such as free lime and C_2S into the melt to form C_3S.

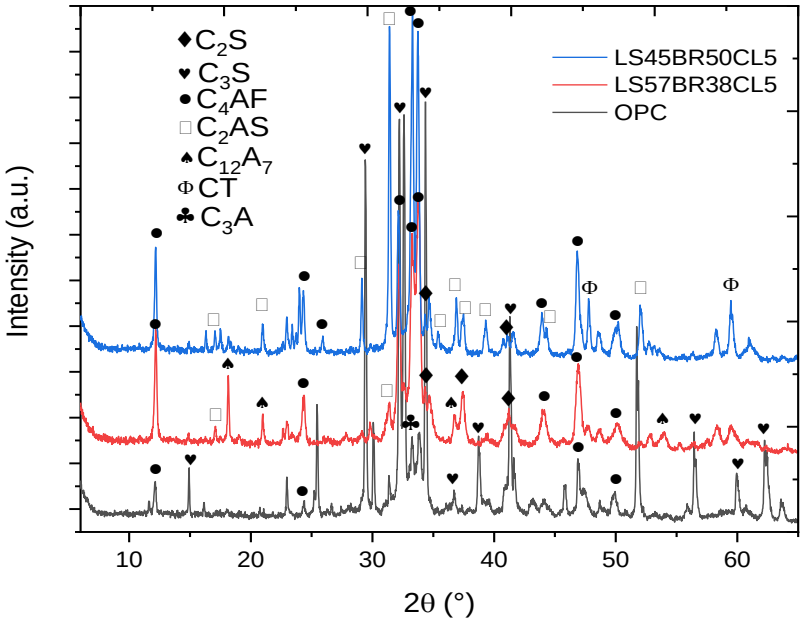

Figure 3. Minerological composition of the cement clinkers.

To further confirm this result, quantitative analysis was done on the following cement clinkers. Using the structures listed in Table 1, the amount of C_2S formed were 18% and 13% with no C_3S present for low BR and high BR ferrite-belite clinker. In the case of OPC, the C_3S and C_2S were 62% and 10% respectively indicating majority of the clinker composition is from the C_3S phase. The low-BR and high-BR clinker mainly comprised of ferrites (66.58 % and 51.88% respectively) as the major phase. Some unreactive phases such as gehlenite was notable when working at

temperatures below 1300°C for the low (7%) and high-BR clinker (20%). In the PhD thesis of Montoya et al. [18], 16% of gehlenite was also reported for the FB clinker constituting 50 wt% LS, 40 wt% BR and 10 wt% K which was one of the probable reason for poor compressive strength of the mortars. Other minor phases such as perovskite (1 % and 13%) and mayenite (7.5% and 1%) were also present in the low-BR and high-BR clinker respectively. The presence of perovskite phases is mainly due to the addition of BR as a raw meal component. Furthermore, with the increased content of BR, the content of gehlenite increases and thus the amount of Al_2O_3 required to form mayenite is insufficient.

3.3 Visualization of the FB Clinkers

The microstructure of the clinker was visually analyzed to differentiate between the clinker phases present. In Figure 4, the low-BR clinker microstructure consisted of a coarsely crystalline ferrite indicated by point '29', and in some places a dark anhedral mayenite (point '24'). The presence of gehlenite (point 28) was also confirmed, indicated by a slight lighter shade in between ferrite and belite shades.

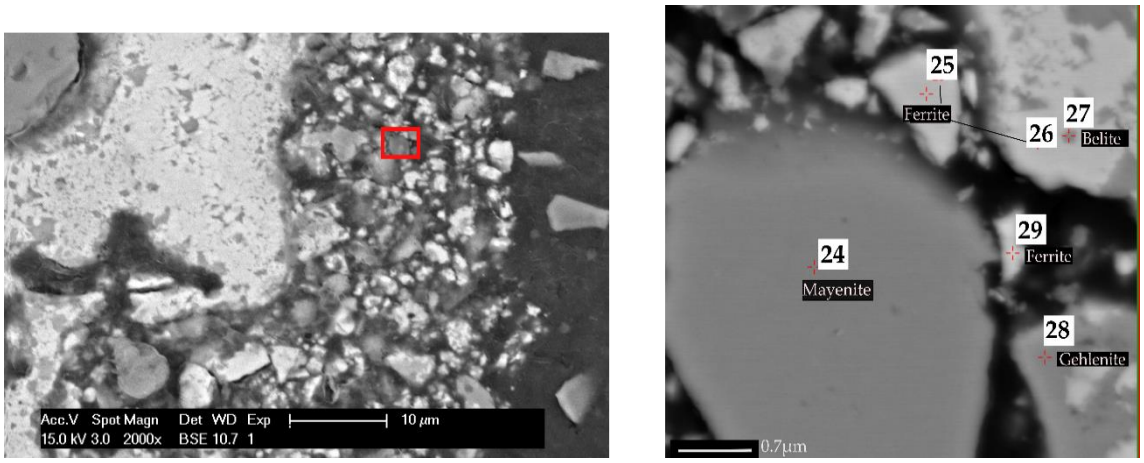

(a) (b)

Figure 4. (a) Backscattered image of low-BR clinker. (b) 5000x magnification of the red frame region in the microstructure.

Figure 5 depicts the backscattered image of the high-BR clinker microstructure. For high-BR clinker microstructure, perovskite could be identified as the brightest shade on the microstructure.

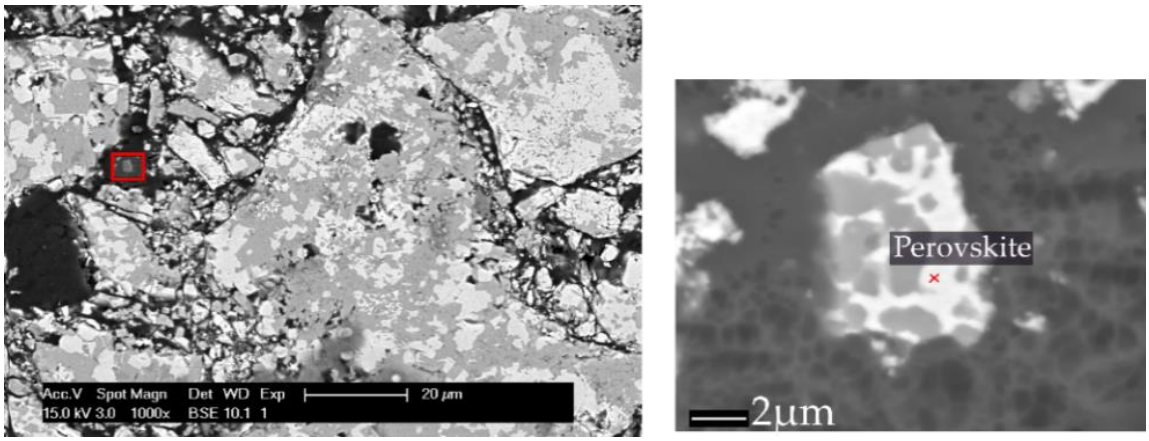

Figure 5. (a) Backscattered image of high-BR clinker. (b) 5000x magnification of the red frame region in the microstructure.

3.4 Chemical Composition and Stoichiometry of the Clinker Phases

Based on the EPMA results, solid solutions of the clinker phases were detected, as shown in Table 4 and Table 5. The composition of belite (C_2S) phases revealed that for low-BR content clinkers, almost pure solid of C_2S phase existed with minor amount of Na^{2+}. The average composition of the belite phase was $C_{1.91}Na_{0.01}S_{0.95.}$ Based on the studies conducted by Morsli et al. [19], presence of Na in belite phase can stabilize the α′H-C_2S and α-C_2S polymorph of belite. This indicates the belites found in this clinker may have a minor content of α′H-C_2S or α-C_2S belite. In the case of high-BR clinker, the belite phase was a solid solution containing stabilizing ions such as Fe^{3+} and Al^{3+}. This is possible due to the rapid cooling of the clinkers after clinkering process and is in agreement with the study conducted by Tantawy et al. [20]. Thus, preventing cracking of the belite crystals due to the inclusion of stabilized ions. The average composition of the belite phase was $C_{2.50}S_{0.92}F_{0.18}A_{0.07}T_{0.04}\ N_{0.03}$.

The ferrite phases in both the clinkers were iron-rich solid solutions. In the case of low-BR clinker, the average composition of the ferrite was $C_{4.11}F_{1.03}A_{0.60}S_{0.56}N_{0.11}T_{0.19}$ whereas for high-BR clinker, the average composition was $C_{3.78}F_{1.01}A_{0.48}S_{0.35}N_{0.02}T_{0.16}$. In the latter case, the stoichiometry of Ca^{2+} ions reduced in the ferrite phase. This is due to the formation of calcium titanium oxide phase (perovskite) which has also presence of some Fe^{3+} ions. Thus, indicating a solid solution between perovskite and ferrite phase. Here the average composition of the perovskite phase was $C_{1.59}A_{0.14}S_{0.14}F_{0.18}N_{0.07}T_{1.02}$. This indicates the perovskite phase formed in the high-BR clinker is more towards its pure phase as mentioned by Gloter et al. [21]. Depending on the reactivity, the ferrite phase in the low-BR clinker had a higher weight fraction of Al_2O_3 (A) than the one present in high-BR clinker. This indicates that the ferrites with higher A/F ratio in the low-BR clinker can have a higher reactivity than the high-BR clinker based on the study conducted by Neubauer et al. [22]. Moreover, the presence of minor amounts of Ti in ferrite phase can be beneficial in terms of compressive strength and reactivity based on the study conducted by Duvallete et al. [23]. It was reported that incorporation of titanium in ferrite phases delayed the production of hydrogarnets (delayed reactivity) thus improving compressive strength after 28 days.

Table 4. Chemical composition of Low-BR ferrite-belite clinker determined by EMPA WDS analysis mol %.

Phase	Al_2O_3 (mol%)	SiO_2 (mol%)	Fe_2O_3 (mol%)	Na_2O (mol%)	CaO (mol%)	TiO_2 (mol%)
C_3FT	4.9±0.2	7.8±0.8	14.4±0.8	0.4±0.4	58.3±0.6	13.9±0.5
C_4AF	9.2±0.5	8.5±0.4	15.1±0.6	1.7±0.4	62.4±0.9	2.9±0.6
$C_{12}A_7$	36.0±0.3	0.6±0.2	1.8±0.5	4.5±0.5	56.7±0.5	0.08±0.0
C_2AS	21.4±0.2	25.3±0.5	3.4±0.2	0.4±0.1	48.3±0.4	1.0±0.0
C_2S	0.1±0.05	34.0±0.4	0.2±0.2	0.3±0.0	65.1±0.5	0.1±0.0

Table 5. Chemical composition of High-BR ferrite-belite clinker determined by EMPA WDS analysis mol%.

Phase	Al_2O_3 (mol%)	SiO_2 (mol%)	Fe_2O_3 (mol%)	Na_2O (mol%)	CaO (mol%)	TiO_2 (mol%)
C4AF	8.3±0.6	6.03±0.4	17.2±0.6	0.4±0.4	65.1±0.8	2.8±0.4
C2S	1.8±0.3	26.1±0.2	4.7±0.5	0.7±0.3	65.4±0.3	1.0±0.3
CT	4.5±0.5	4.7±0.5	5.9±0.5	2.9±0.1	50.7±0.4	31.8±0.3
C2AS	16.0±0.2	22.2±0.9	5.28±0.2	0.5±0.1	55.3±0.6	0.6±0.0

4. Conclusion

Based on the characterization of the FB cement clinker, the gehlenite content increases with higher BR content in raw meal of FB clinkers. Moreover, high gehlenite content also diminishes the mayenite that formed at low temperatures (at temperatures < 1300°C). Hence in the high-BR clinker, the mayenite formation was suppressed due to increased gehlenite content in comparison to low-BR clinker. Furthermore, the content of belite in FB-clinkers where higher than the OPC and this is due to the absence of melt formation when sintering at lower temperatures. The chemical composition of the clinker phases revealed that most of the reactive phases such as belite and ferrites were stabilized by metal ions due to rapid cooling of the clinkers. Moreover, the BR content in the raw meal influenced the A/F ratio in the ferrite phase i.e., higher the BR content, lower the A/F ratio and thus reduced reactivity of the ferrite phase. This change in the A/F stoichiometry and the stabilization of the phases can improve the reaction kinetics during hydration of the cement. However, new strategies need to be devised in order to control the content of gehlenite in these clinkers, which are unreactive and do not contribute to the strength of the cement. Thus, raw materials that contain very high alumina and minor amounts of silica can be used with BR to formulate such clinkers.

5. References

1. Ken Evans, The History, Challenges, and New Developments in the Management and Use of Bauxite Residue. *Journal of Sustainable Metallurgy*, 2016. **2**(4): p. 316-331.
2. Quentin D. Avery et al., Bauxite Residue/Red Mud, in *Smelter Grade Alumina from Bauxite: History, Best Practices, and Future Challenges*, B.E. Raahauge and F.S. Williams, Editors. 2022, Springer International Publishing: Cham. p. 269-338.
3. Technology Roadmap – Maximizing the use of Bauxite Residue in Cement, *International Aluminium Institute (2020)*, https://international-aluminium.org/resource/technology-roadmap-maximizing-the-use-of-bauxite-residue-in-cement/ (accessed on 19 April 2022).
4. Xiao Wang et al., Utilization of red mud as raw material in the production of field road cement. *Journal of Wuhan University of Technology-Mater. Sci. Ed*., 2016. **31**(4): p. 877-882.
5. Michiel Giels et al., High performance mortars from vitrified bauxite residue; the quest for the optimal chemistry and processing conditions. *Cement and Concrete Research*, 2022. **155**: p. 106739.
6. David Ariño-Montoya et al., From bauxite residue to calcium sulfo-ferroaluminate cement: Study of the clinkerization and hydration kynetics. *Proceedings of 12th Panhellenic Scientific Conference of Chemical Engineering, Athens, 29-31 May 2019*.
7. Tobias Hertel et al., Boosting the use of bauxite residue (red mud) in cement - Production of an Fe-rich calciumsulfoaluminate-ferrite clinker and characterisation of the hydration. *Cement and Concrete Research*, 2021. **145**: p. 106463.
8. David Ariño-Montoya et al., Low-Carbon Footprint Cements Incorporating High Volumes of Bauxite Residue in *Proceedings of 35th International ICSOBA Conference*. 2017. Hamburg, Germany.
9. Rahul Roy, Tobias Hertel, and Yiannis Pontikes, *Use of bauxite residue as raw material for low-carbon ferrite-belite cements: prediction of the crystalline phases using thermodynamic modelling*. 2022. in Proceedings of 39th International ICSOBA Conference. 2017. Manama, Bahrain.
10. Koumpouri, D, et al. "Effect of Clinkering Conditions on Phase Evolution and Microstructure of Belite Calcium-Sulpho-Aluminate Cement Clinker." Cement and Concrete Research, vol. 147, 2021, p. 106529.
11. Snellings, R., et al., Rietveld Refinement strategy for quantitative phase analysis of partially amorphous zeolitized tuffaceous rocks. Geologica Belgica, 2010. 133: p. 183-196.
12. Colville, A.A. and S. Geller, The crystal structure of brownmillerite, Ca2FeAlO5. Acta Crystallographica Section B, 1971. 27(12): p. 2311-2315.

13. Mumme, W.G., et al., Rietveld crystal structure refinements, crystal chemistry and calculated powder diffraction data for the polymorphs of dicalcium silicate and related phases. N. Jb. Miner. Abh., 1995. 169(1): p. 35-68.
14. Gemmi, M., et al., Non-ideality and defectivity of the åkermanite-gehlenite solid solution: An X-ray diffraction and TEM study. American Mineralogist, 2007. 92(10): p. 1685-1694.
15. Sakakura, T., et al., Determination of the local structure of a cage with an oxygen ion in Ca12Al14O33. Acta Crystallographica Section B: Structural Science, 2011. 67(3): p. 193-204.
16. Rodríguez-Carvajal, J., M. Vallet-Regí, and J.M.G. Calbet, Perovskite threefold superlattices: A structure determination of the A3M3O8 phase. Materials Research Bulletin, 1989. 24(4): p. 423-430.
17. Lawrence, C.D., *8 - Physicochemical and Mechanical Properties of Portland Cements*, in *Lea's Chemistry of Cement and Concrete (Fourth Edition)*, P.C. Hewlett, Editor. 1998, Butterworth-Heinemann: Oxford. p. 343-419.
18. Arino Montoya, David. Fe-Rich Hydraulic Binders from Bauxite Residue. PhD Thesis 2022.
19. Morsli, K., et al., Mineralogical phase analysis of alkali and sulfate bearing belite rich laboratory clinkers. Cement and Concrete Research, 2007. 37(5): p. 639-646.
20. Tantawy, M.A., et al., *Low Temperature Synthesis of Belite Cement Based on Silica Fume and Lime.* International scholarly research notices, 2014. **2014**: p. 873215-873215.
21. Gloter, A., et al., *TEM evidence of perovskite–brownmillerite coexistence in the Ca(AlxFe1−x)O2.5 system with minor amounts of titanium and silicon.* Physics and Chemistry of Minerals, 2000. **27**(7): p. 504-513.
22. Neubauer, J., F. Goetz-Neunhoeffer, and I. Lindner, *Investigation of hydration behaviour of ferrite phase C6AxF3-y with different Al3 +-content in mixes with C3A and gypsum using a revised highly efficient isothermal calorimeter*. Proceedings of the 11th International Congress on the Chemistry of Cement, Durban 2003 (South Africa), 2004. **1**: p. 641-656.
23. Duvallet, T., T.L. Robl, and F.P. Glasser, *The effect of titanium dioxide on the structure and reactivity of ferrite, 8th international conference: concrete in the Low Carbon Era, Dundee*. UK, 2012: p. 584-593.